# Design, Synthesis, and Characterization of a −Donor−Bridge−Acceptor−Bridge- Type Block Copolymer via Alkoxy- and Sulfone- Derivatized Poly(phenylenevinylenes)

**Cheng Zhang,[†] Soobum Choi,[†] James Haliburton,[†] Taina Cleveland,[†] Rui Li,[†] Sam-Shajing Sun,*[,†,‡] Abram Ledbetter,[†] and Carl E. Bonner[†,‡]**

*Center for Materials Research and Chemistry Department, Norfolk State University, 700 Park Avenue, Norfolk, Virginia 23504*

*Received January 24, 2006; Revised Manuscript Received May 2, 2006*

ABSTRACT: A novel class of light harvesting conjugated block copolymers, with electron-donating conjugated blocks (**D**) connected to electron-accepting conjugated blocks (**A**) via non conjugated and flexible bridge chains (B), has been designed, synthesized, and characterized. Specifically, **D** is a decyloxy-substituted polyphenylenevinylene ($C_{10}$−PPV). $\mathbf{A_1}$ and $\mathbf{A_2}$ are PPVs with sulfone ($SO_2$) acceptor moieties substituted on every other phenylene unit. $\mathbf{A_1}$ carries two decyloxy groups on every phenylene unit, while in $\mathbf{A_2}$, half of the phenylene units are unsubstituted. The optical energy gaps are 2.24 eV for the donor block (**D**), 2.33 and 2.45 eV for $\mathbf{A_1}$ and $\mathbf{A_2}$ acceptor blocks. LUMO level offsets are 0.24 and 0.16 eV for $\mathbf{D}/\mathbf{A_1}$ and $\mathbf{D}/\mathbf{A_2}$ pairs, respectively. Comparing the photoluminescence from both films and solutions, very large red shifts (71 and 74 nm for $\mathbf{A_1}$ and $\mathbf{A_2}$ respectively) were observed in the two acceptor polymers. These red shifts in the emission spectra were more than twice as much as that observed for **D** (31 nm). The $(\mathbf{DBA_1B})_n$ and $(\mathbf{DBA_2B})_n$ block copolymer films exhibited improved processability and optoelectronic properties when compared with the corresponding films composed of donor/acceptor blends. Atomic force microscopic (AFM) studies of **D**, $\mathbf{A_1}$, and $\mathbf{A_2}$ films were also undertaken to observe the degree of aggregation in the films. The results indicate the tendency of intermolecular aggregation increases as $\mathbf{A_2} > \mathbf{D} > \mathbf{A_1}$. AFM topological images revealed that large aggregates of several hundreds of nanometers formed in donor/acceptor blend films, while in block copolymer films, domain sizes were similar to individual block sizes which are 1 order of magnitude smaller than in the blend.

## Introduction

Since an organic small molecule electron donor/acceptor bilayer heterojunction solar cell was reported in 1986,[1] the energy conversion efficiency of organic and polymeric solar cell has been improved by various chemical and engineering approaches.[2] Major progress was achieved by replacing the bilayer (e.g. MEH−PPV/C60)[3] with a physical blend,[2,4−6] where the electron donor and electron acceptor interact in the entire volume of the composite film to form a "bulk heterojunction" . The ideal bulk heterojunction requires the morphology of donor/acceptor binary system to be two continuous phases where each phase has a size on the order of the average exciton diffusion length, usually less than 100 nm.[2] A great amount of research effort has been conducted to optimize the donor/acceptor blend morphology by changing thin film processing conditions, including solvent and annealing conditions.[6] Although significant improvement has been obtained in such donor/acceptor blend systems, the perfect nanoscale ordered morphology may not be achievable in simple physical blends of polymers for several reasons. The first reason is due to the incompatibility of materials. For incompatible materials (e.g., polymer/polymer or polymer/$C_{60}$ derivatives), nanoscale phase-separated states are still high in energy due to extremely large interfacial area, i.e. the desired nanosize morphology is likely unstable under operational conditions. A second reason is due to the balance of conditions required to control the morphology of the blends. The phase separation in a polymer blend is a dynamically controlled process, and is therefore highly dependent on processing conditions, which results in low repeatability. Finally, the phase separation in a blend is statistical, and results in a wide range of domain sizes from micrometers to nanometers all at the same time.

It is natural to think of a single material where conjugated donor and acceptor blocks are covalently linked by nonconjugated chains, and where physically different donor and acceptor blocks may undergo phase separation on the nanometer scale. This type of arrangement is well-known in many block copolymers.[7] A desired morphology may be achieved via judicial design of the chemical structure of the materials. The phase separation of such block copolymers will be fundamentally distinct from that of a physical blend for the following reasons. First, the covalent bonding dictates that phase separation in such material must be on the same scale as the size of building blocks. Second, the phase-separated state is stable because the covalent bonding will not allow the separation to go beyond this limit. Finally, the morphology in the equilibrium state can be tuned via molecular engineering of bridge length, volume ratio, side groups, and size of the blocks.[7]

A number of studies have already been conducted along this scientific direction using two main approaches, e.g., (1) double-cable polymers where electron acceptors, such as $C_{60}$ or anthraquinone units are attached to conjugated polymers to form a donor−acceptor "double cable"[8−10] or (2) block copolymers where a poly(*p*-phenylenevinylene) (PPV) electron-donating block is covalently linked to a $C_{60}$-bearing polystyrene block [i.e. PPV-*b*-P(S-*stat*-$C_{60}$MS)].[11] Although some promising properties have been observed in solutions and thin films, such as lamellar organization of anthraquinone−PT double cable in films and nanometer-scale aggregation in block copolymer films,

[†] Center for Materials Research, Norfolk State University.
[‡] Chemistry Department, Norfolk State University.

10.1021/ma060179j CCC: $33.50 
Published on Web 06/03/2006

the potential of covalently linked D−A macromolecular systems for photovoltaic applications still remains to be fully demonstrated.

Over the past several years, we have been developing a light harvesting block copolymer focusing on a different and unique structural system.[12−14] Specifically, we have been developing a $(\mathbf{DBAB})_n$-type block copolymer, where **D** is a conjugated donor block, **A** is a conjugated acceptor block, and **B** is a nonconjugated bridge connecting **D** and **A**. The lack of conjugation in the bridge is to separate the electronic states of the donor from the acceptor and to slow the intramolecular charge recombination. It has been shown that no photoinduced charge separation was observed in a D−A copolymer where the donor and acceptor blocks are directly linked, possibly due to ultrafast charge recombination.[15]

Both PPV and polythiophene[16] based donor/acceptor end functionalized polymer blocks have been explored, yet only PPV-based $(\mathbf{DBAB})_n$ block copolymer system have been fully studied so far. In our PPV-based $(\mathbf{DBAB})_n$ block copolymer design, the **A** block is very similar to the **D** block in terms of rigidity and cross-sectional dimensions as well as its structural composition. In contrast, in previously reported PPV-*b*-P(S-*stat*-$C_{60}$MS),[11] the acceptor block bears no such resemblance to the PPV block. The structural similarity between **D** and **A** in our system is expected to yield improved orbital overlap between the $\pi$ orbitals on the donor and acceptor blocks or so-called "$\pi-\pi$ stacking". In this paper, we report details of material synthesis, chemical and spectroscopic characterizations, and some morphological studies of this novel class of block copolymers.

## Experimental Section

**Starting Materials, Instrumentation, and General Methods.** All starting materials, reagents and solvents were purchased from commercial sources (mostly from Sigma-Aldrich and Fisher-Scientific) and used without further purification. NMR spectral data was obtained from a Bruker Avance 300 MHz spectrometer with TMS as the internal reference. Elemental analysis was performed by Atlantic Microlab Inc. UV−vis data was collected on a Varian Cary-5 spectrophotometer. Luminescence spectra were obtained from an ISA Fluoromax-3 luminescence spectrofluorometer. Thermal analysis was performed on a Perkin-Elmer TGA6/DSC6 system. Polymer film thicknesses were measured with a Dektak-6M profilometer.

**Gel Permeation Chromatography.** The polymer molecular weights were measured on a Viscotek T60A/LR40 triple-detector GPC system at ambient temperature. Polystyrene standards were used for universal calibration. Although $CHCl_3$ is a better solvent than tetrahydrofuran (THF) for PPVs, its refractive index (RI = 1.446) is too high, leading to very weak refractive index (RI) detector signal. THF, with a RI of 1.405 is used for all materials measured by GPC.

**Cyclovoltammetry.** Electrochemical studies were performed on a Bioanalytical (BAS) Epsilon-100w tri-electrode cell system. Three electrodes are a glassy carbon working electrode, an ancillary Pt electrode, and a silver reference electrode (in a $CH_3CN$ solution of 0.01 M $AgNO_3$ and 0.1 M TBA-HFP). The polymer samples were dissolved at a concentration of 0.1 mM (based on average MW of polymer, not a repeating unit) in anhydrous THF with 0.10 M tetrabutylammonium hexafluorophosphate (TBA−HFP). Ferrocene (2 mM in 0.10 M TBA−HFP/THF solution) was used as an internal reference standard (its HOMO level of −4.8 eV was used in calculations). Before starting a measurement, dry nitrogen gas was bubbled through the solution for at least 10 min to remove any dissolved oxygen. Between the experiments, the surface of the electrodes were cleaned or polished. Scan rate was 100 mV/s. AFM images were taken on a Nanoscope IV microscope (Digital Instruments Veeco Co.) in the standard tapping mode with multipurpose cantilever.

**[2,5-Bis(decyloxy-4-(diethoxyphosphorylmethyl))benzyl]phosphonic Acid Diethyl Ester (5).** A mixture of 1,4-Bis(*n*-decyloxy)-2,5-di(bromomethyl)benzene (15.00 g, 26.02 mmol) and triethyl phosphite (8.7 g, 65.05 mmol) was stirred at 130 °C for 3 h. The remaining triethyl phosphite was removed by vacuum suction at 175−180 °C. A total of 17.8 g of white solid was obtained. Yield: 99%. $^1$H NMR ($CDCl_3$): $\delta$ 6.92, 4.02 (8H, quintet, J 7.15 Hz), 3.92 (4H, triplet, J 6.5 Hz), 3.23 (4H, doublet, J 20.18 Hz), 1.77 (4H, q, J 6.54 Hz), 1.45 (4H, q, J 7.08 Hz), 1.24 (34H, mult.), 0.88 (6H, t, J 6.89 Hz). $^{13}$C NMR: 150.72, 119.81, 115.27, 69.55, 62.15, 32.21, 29.92, 29.88, 29.80, 29.76, 29.64, 26.59 (doublet at 27.51 and 25.67, J 38.96 Hz), 26.46, 16.67 (t, $J$ = 3.0 Hz), 14.40. Anal. Calcd for $C_{36}H_{68}O_8P_2$: C, 62.59; H, 9.92. Found: C, 62.69; H, 10.11.

**1-Decyloxy-4-decylsulfanylbenzene (6).** A solution of 4-mercaptophenol (12.62 g, 0.1 mol), potassium hydroxide (12.9 g, 0.23 mol), and deionized water (15 mL) in acetonitrile (400 mL) was heated to 80 °C. Next, 1-bromodecane (44.24 g, 0.2 mol) was added. After reacting overnight, the mixture was poured into deionized water (∼800 mL). The solid was collected by filtration and then dissolved in a small amount of chloroform (∼20 mL), and then reprecipitated in cold methanol (∼800 mL). Solid was filtered again and allowed to dry. Yield: 90%. $^1$H NMR ($CDCl_3$): 0.88 (t, 6H, J 6.1 Hz), 1.27 (m, 28H), 1.57 (quintet, 2H, J 7.0 Hz), 1.76 (quintet, 2H, J 7.0 Hz), 2.80 (t, 2H, J 7.3 Hz), 3.92 (t, 2H, J 6.5 Hz), 6.82 (d, 2H, J 8.3 Hz), 7.31 (d, 2H, J 8.3 Hz). Anal. Calcd for $C_{26}H_{46}$-OS: C, 76.78; H, 11.40. Found: C, 76.76; H, 11.43.

**1,4-Bis(bromomethyl)-2-decyloxy-5-decylsulfanyl benzene (7).** A solution of **6** (10.17 g, 25 mmol) and paraformaldehyde (in excess, 4.0 g) in formic acid (75 mL) was heated to, and maintained at, 68 °C. Next, fresh 33% HBr/acetic acid (60 mL) was added. After reacting for 3 days, the mixture was cooled to room temperature, poured into deionized water (∼800 mL), then vacuum filtered. The Solid was then dissolved in a small amount of chloroform (8−10 mL), and reprecipitated in cold methanol (∼800 mL). Solid was collected by filtration and dried in vacuo. Yield: 70%. $^1$H NMR ($CDCl_3$): $\delta$ 0.88 (t, 6H, J 6.1 Hz), 1.27 (m, 28H), 1.57 (quintet, 2H, J 7.0 Hz), 1.76 (quintet, 2H, J 7.0 Hz), 2.85 (t, 2H, J 7.2 Hz), 4.03 (t, 2H, J 6.3 Hz), 4.50 (s, 2H), 4.72 (s, 2H), 6.92 (s, 1H), 7.42 (s, 1H). Anal. Calcd for $C_{28}H_{48}Br_2OS$: C, 56.75; H, 8.16. Found: C, 56.50; H, 8.28.

**[5-(Decyloxy-2-decylsulfanyl-4-(diethoxyphosphorylmethyl))-benzyl]phosphonic Acid Diethyl Ester (8).** Triethyl phosphite (4.98 g, 30 mmol) and **7** (8.89 g, 15 mmol) were mixed and heated to 120 °C under a nitrogen atmosphere. Reaction was stopped after 24 h and no further purification was needed. Yield: 100%. $^1$H NMR ($CDCl_3$): $\delta$ 0.88 (t, 6H, J 6.1 Hz), 1.27 (m, 40H), 1.57 (quintet, 2H, J 7.0 Hz), 2.77 (t, 2H, J 7.0 Hz), 3.21 (d, 2H, J 20.7 Hz), 3.52 (d, 2H, J 21.7 Hz), 4.02 (m, 10H), 7.00 (s, 1H), 7.45 (s, 1H). Anal. Calcd for $C_{36}H_{68}O_7P_2S$: C, 61.16; H, 9.70. Found: C, 60.87; H, 9.82.

**[2-(Decane-1-sulfonyl)-5-(decyloxy 4-(diethoxyphosphoryl-methyl))benzyl]phosphonic Acid Diethyl Ester (9).** 50% Hydrogen peroxide (4.0 g) and **8** (10.16 g, 14 mmol) were dissolved in glacial acetic acid (40 mL). The mixture was heated to 130 °C and refluxed for 48 h. Solvent was then removed by rotary evaporation. Further purification was performed with column chromatography (1:2, acetone:hexane as eluent). Yield: 70%. $^1$H NMR ($CDCl_3$): $\delta$ 0.88 (m, 6H), 1.27 (m, 40H), 1.73 (q, 2H, J 7.0 Hz), 1.83 (q, 2H, J 7.0 Hz), 3.25 (d, 2H, J 22.8 Hz), 3.27 (t, 2H, J 7.9 Hz), 3.81 (d, 2H, J 21.9 Hz), 4.08 (m, 10H), 7.13 (s, 1H), 7.93 (s, 1H). $^{13}$C NMR: $\delta$ 14.3, 16.7, 22.8, 25.7, 26.0, 27.6, 28.4, 28.9, 29.1, 29.4, 30.8, 31.8, 57.4, 62.5, 69.3, 115.4, 120.7, 129.5, 133.2, 134.2, 160.4. Anal. Calcd for $C_{36}H_{68}O_9P_2S$: C, 58.51; H, 9.28. Found: C, 58.74; H, 9.30.

**1,2-Bis(4-formylphenoxy)ethane.** A mixture of *p*-hydroxybenzaldehyde (32.5 g, 0.266 mol), 1,2-dibromoethane (94.7 g, 0.134 mol), DMSO (anhydrous, 300 mL), and NaOH powder (40.51 g, 0.269 mol) was stirred in a 10 °C water bath for 1 h, then at room

**Scheme 1. Synthetic Scheme of the Donor Block D**

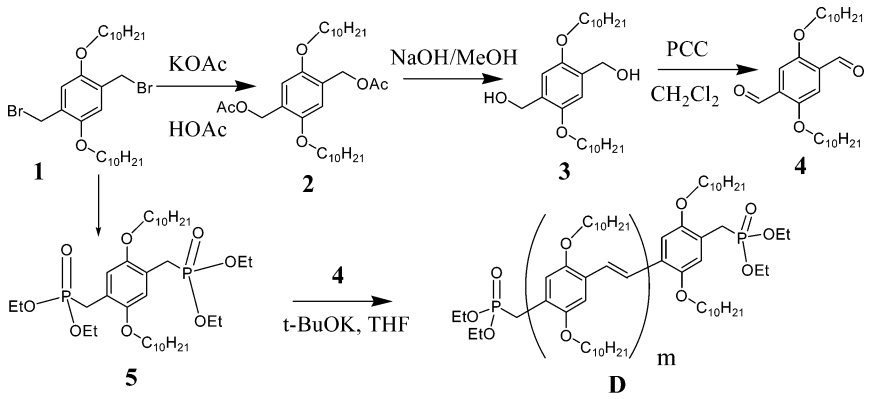


temperature for 24 h, and finally at 50 °C for 7 h. After the reaction was cooled to room temperature, ether was added. The resulting mixture was washed with water. The crude product was purified with a silica gel column to afford 15.8 g light brown crystal. Yield 44%. $^1$H NMR and $^{13}$C NMR data are identical to the literature data.[21]

**Stability Test of 2,5-Bis(decyloxy-1,4-benzene)dicarboxaldehyde (4).** In a drybox, 5 mL of THF was added to a mixture of 120 mg of 4 and 200 mg of *t*-BuOK. The solution was stirred for 7 min at room temperature. It was then quenched by adding dilute hydrochloric acid to pH = 6−8. See Supporting Information for details on decomposition products separation/analysis and mechanism discussion.

**Donor Block D (Dialdehyde/Diphosphonate = 15/16).** To a solution of **5** (1.842 g, 2.6667 mmol) and **4** (1.117 g, 2.5 mmol) in THF (20 mL) in a drybox was added *t*-BuOK(5.866 mmol, in 20 mL of THF) over 2 min. After being stirred for 8 min, the solution was neutralized with a few drops of acetic acid and then dropped into 300 mL of methanol. Then 2.1 g of red polymer solid was obtained after filtration, methanol washing, and vacuum-drying. Yield: 95%.

**BDB.** In a drybox, a mixture of **D** (0.700 g, 0.0533 mmol), 1,2-bis(4-formylphenoxy)ethane (0.288 g, 1.066 mmol) and THF (10 mL) was heated to boil for a few minutes until it became a homogeneous solution. We waited 5 min to allow the solution to cool. *t*-BuOK (23.9 mg, 0.213 mmol, in 1 mL of THF) was added all at once. Then, 30 s later, the reaction mixture was quenched with 0.2 mL of acetic acid and then dropped into stirred MeOH (75 mL). The red polymer powder was collected by filtration, washed with MeOH, and dried in vacuo: 0.676 g, 93% yield.

**Acceptor Block $A_1$ (Diphosphonate:Dialdehyde = 16:15).** To a stirred mixture of **9** (1.500 g, 2.030 mmol), **4** (850 mg, 1.903 mmol) and THF (20 mL) was added a solution of *t*-BuOK (470 mg, 4.187 mmol) in THF (15 mL) over 5 min. The solution was stirred for another 5 min, and was then quenched with acetic acid. The mixture was dropped into stirred MeOH (220 mL). The orange polymer was collected by filtration, washed with MeOH, and dried in vacuo: 1.688 g, yield 95.7%.

**Acceptor Block $A_2$ (Diphosphonate:Dialdehyde = 9:8).** To a stirred mixture of **9** (3.166 g, 4.284 mmol), 1,4-benzenedicarbaldehyde (510.8 mg, 3.808 mmol), and THF (30 mL) was added a solution of *t*-BuOK (1.054 g, 9.43 mmol) in THF (10 mL) over 5 min. The solution was stirred for another 5 min and then quenched with acetic acid. The mixture was dropped into MeOH. The orange product was collected by filtration, washed with MeOH, and dried in vacuo: 1.644 g, yield 65.8%.

**Block Copolymer $(DBA_1B)_n$:** In a drybox, **BDB** (0.550 g, 0.0411 mmol) and $\mathbf{A_1}$ (0.0493 mmol, 0.6853 g) were dissolved in 12 mL of boiling THF. The solution was allowed to cool. When it started to turn cloudy, a solution of *t*-BuOK(0.197 mmol, 24 mg) in 1 mL of THF was added over 2 min. The solution became very viscous due to the formation of high MW polymer. Stirring was continued for 8 min, and the solution was dropped into MeOH (70 mL). The red solid was collected by filtration, washed with MeOH, and dried in vacuo: 1.208 g, yield 98%.

**Block Copolymer $(DBA_2B)_n$:** In a drybox, **BDB** (0.6 g, 0.04484 mmol), $\mathbf{A_2}$ (0.2829 g, 0.0538 mmol) and THF (12 mL) are placed in a 50 mL round-bottom flask. The mixture was heated to boiling with a heat gun. Some polymer (presumably the acceptor block, because **DBD** could not fully dissolved) remained undissolved and stuck to the wall of the vessel. The mixture was allowed to cool for 5 min, and then *t*-BuOK (24 mg in 2 mL of THF) was added in portions over 30 min. The reaction mixture (not including the solid on the wall) was dropped into MeOH, The red solid was collected by filtration, washed with MeOH, and dried in vacuo: 0.784 g. Yield: 90.5%.

## Results and Discussion

The synthesis of the $(\mathbf{DBAB})_n$ conjugated block copolymer involves three key steps: (1) synthesis of end-functionalized conjugated donor block (**D**), (2) synthesis of end-functionalized conjugated acceptor block (**A**), and (3) integration of the conjugated donor and acceptor blocks into the final $(\mathbf{DBAB})_n$ block copolymer via a non conjugated and flexible bridge unit. The synthetic schemes for **D**, **A**, and final $(\mathbf{DBAB})_n$ are shown in Schemes 1−3 and discussed in detail below.

**Molecular Weight Control, Calculations, and Measurements.** The control of the size of **D** and **A** blocks is critical since the size of these domains should not be too much greater than the average exciton diffusion lengths, which are estimated to be around 10 nm for PPV.[2,21] For a condensation polymer reaction using two difunctional monomers, polymerization degree [$N(t)$, t means theoretical] can be calculated from the equation[23]

$$N(t) = \frac{1+R}{1+R-2Rp} = \frac{1+R}{1-R} \qquad (1)$$

where $R$ is the molar ratio between two monomers, $N_A/N_B$, with monomer B in excess ($N_A < N_B$), and $p$ is the extent of reaction, defined as the fraction of monomer A that has reacted at a particular time.

The polymerization in the scheme and presented in this work is based on the Horner−Emmons coupling reaction for producing carbon−carbon double bond from a phosphonate and an aldehyde. This reaction appears ideal for constructing desired end-functionalized PPV blocks as it was used in our earlier synthesis of second-order nonlinear optical chromophores[17,18] and similar PPVs.[12−14,19] Selection of the base (to produce the reactive anion from phosphonates) is critical since, as was shown previously, it was difficult to obtain a desired molecular weight when NaH was used due to the slow reaction rate and low polymer yields.[12−14] When *t*-BuOK was used in place of NaH,

**Scheme 2. Synthetic Scheme of the Acceptor Blocks $A_1$ and $A_2$**

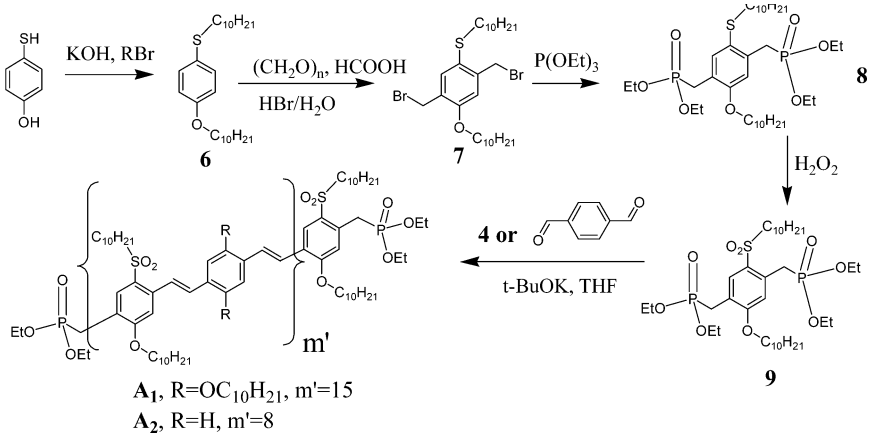


**Scheme 3. Synthetic Scheme of the Block Copolymers $(DBA_1B)_n$ and $(DBA_2B)_n$, Where Only the Chemical Structure of $(DBA_2B)_n$ Is Shown**

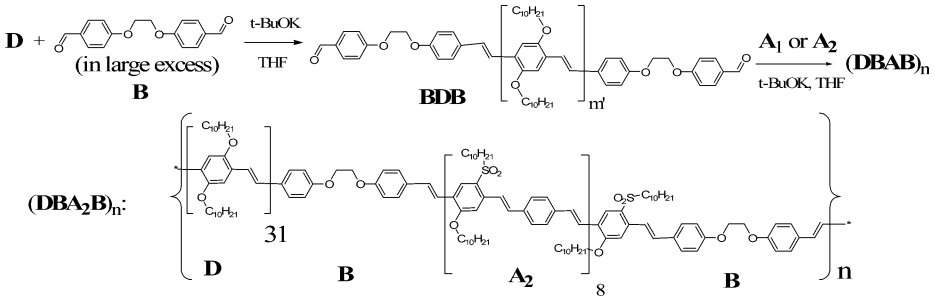


the polymerizations were completed in a few minutes instead of a few days, and high yields (95−99%) of polymers are obtained after the routine precipitation in methanol. Equation 1 can be used to predict molecular weight. As an example, if $n$ moles of monomer A and $n + 1$ moles of monomer B are used in the reaction, $N(t) = 2n + 1$. Thus, a monomer ratio of dialdehyde:diphosphonate = 15:16 would lead a PPV block containing 31 phenylene units and end functionalized with phosphonates.

Impurities of any kind, such as moisture, dust, side products, residual solvents, or a boiling chip, can render the molecular weight control ineffective. As an example, to prepare a PPV with 31 phenylene units using the dialdehyde (100% pure) and the diphosphonate (99% purity), a 1% impurity (assumed to be inert) turns the designed monomer ratio of 15:16 to an actual ratio of 15:15.84. Let $15:15.84 = n:(n + 1)$; we obtain $n = 17.86$. According to the analysis in the last paragraph, we will get a PPV with $2n + 1 = 36.7$ phenylene units on average. Similar calculations show that a 2% of impurity in the diphosphonate will lead to a PPV block with 45.1 phenylenevinylene units. It is clear that an effective control of molecular weight requires nearly 100% pure of monomers. Therefore, the monomers and the bridge compound were purified very carefully using column chromatography and/or recrystallization until satisfying NMR and elemental analysis results are both obtained.

**Synthesis of the Donor Block (D).** Decyloxy-substituted benzenedicaboxaldehyde **4** was synthesized according to the literature procedures.[20] Another monomer, diphosphonate **5** was synthesized in one step from homemade dibromide **1** in a quantitative yield. Before **4** and **5** were used for the donor block preparation, their chemical stabilities were examined under the condition of the Horner−Emmons reaction. While **5** was found to be stable, **4** was decomposed 100% into more than one species after 7 min in *t*-BuOK/THF solution at room temperature. (see Experimental Section for the detail of the test, and pages 1−6 in the Supporting Information for decomposition product analysis and mechanism discussion) Although the decomposition reaction of the dialdehyde is very fast, the harm to the polymer formation can be minimized by adding the base *t*-BuOK/THF dropwise, so that the base is never in excess until the end of polymerization reaction. On the basis of the previous successful synthesis of high molecular weight PPV using this strategy, we have deduced that the deprotonation of the active methylene groups in the diphosphonate **5** is much faster than the decomposition of the dialdehyde. To eliminate the possibility of damage to the end group, we have used a slight excess of diphosphonate **4** so that the resulting PPV was end-capped with phosphonate groups. This was necessary since the phosphonate (in the deprotonated form in the presence of *t*-BuOK) is stable under the reaction condition. It was also observed later that the phosphonate end groups also significantly improve the solubility. From the $^1$H NMR spectrum of **D** (Figure 1), it is clear that the reaction between the two monomers was complete as the aldehyde peak is no longer observed. The presence of phosphonate end group is evidenced through the doublet peak of the methylene protons. The integration ratio of the methylene proton (at 3.2 ppm) to aromatic protons (including the vinylene protons) is about 3:122. Since 4% of the polymer (presumably of low molecular weight) was lost to precipitation in methanol, the expected ratio should be smaller than the theoretical ratio of (4:122). Assuming the lost fraction has an average molecular weight of one-fourth of the MW of the whole product, the end group lost in this purification process accounts for 16% of the total end groups. As a result, the proton ratio changes from 4:122 to 3.5:122. Considering the relatively large uncertainty in the integration of the weak methylene proton peak, the measured ratio is in fact quite close to the expected ratio. Two peaks show up for the first methylene protons ($OC\mathbf{H}_2C_9H_{19}$). The peak at 4.08 ppm is from the structural unit having a trans C═C double bond as shown in Figure 1. This assignment is made on the

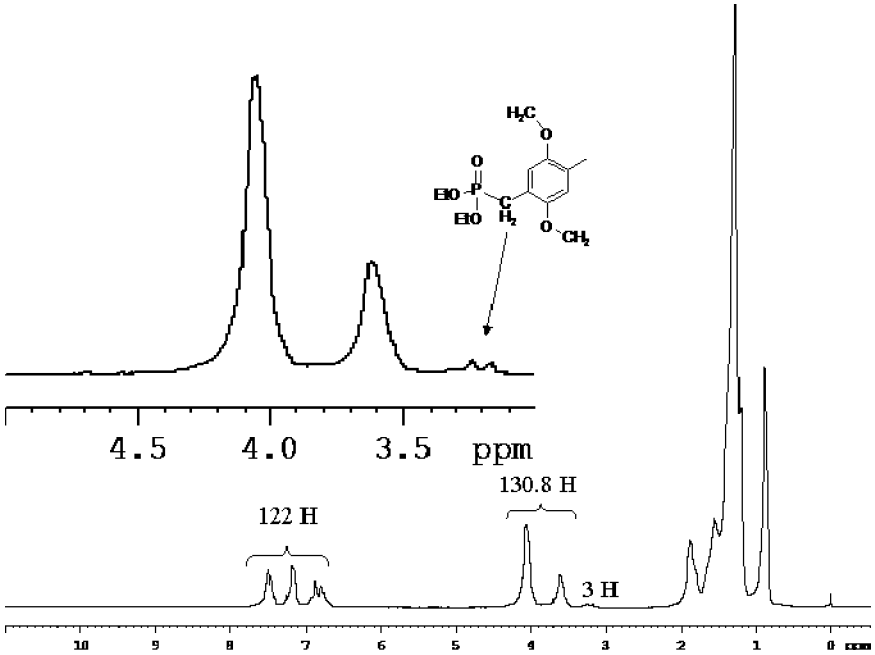


**Figure 1.** $^1$H NMR of the donor block (**D**) in $CDCl_3$. The inset spectrum shows the enlarged spectral region between 3 and 5 ppm. The chemical structure shows one of the phosphonate-terminated ends of of **D**.

basis of the $^1$H NMR spectrum of a structurally similar commercial polymer, poly[2,5-bisoctyloxy-1,4-phenylenevinylene (Aldrich Chem. Co.). And the peak at 3.61 ppm is from the structural unit having a cis C═C double bond. The shift of the cis peak to the higher field (relative to the trans peak) is due to the shielding effect of phenyl ring in the crowded cis structure unit. The ratio of the two peaks is 72:28 (trans:cis), and is almost a constant for all donor blocks of different length and different side chain ($C_6$, $C_8$, $C_{10}$,) synthesized in our lab. The cis C═C double bond can be transformed into trans by boiling with $I_2$ in chloroform solution as evidenced by the disappearance of the cis peak and enhancement of the trans peak.[20] However, this treatment causes some degree of degradation of the polymer. Therefore, the polymers (including **A** and final block copolymers) were used without isomerization treatment.

**The Synthesis of the Acceptor Blocks $A_1$ and $A_2$.** Two different acceptor blocks were designed and synthesized. The sulfone-bearing monomer **9** was used in the synthesis of both. Bromomethylation of 1-decyloxy-4-decylsulfanylbenzene **6** turned out to be much more difficult than that of 1,4-bis-(decyloxy)benzene which always proceeded smoothly and gave a quantitative yield. This may be attributed to the bigger steric hindrance and weaker electron donating ability of the SR as compared to the OR. It was found that the reaction can be effected in a 70% yield by using formic acid as the solvent instead of acetic acid.

A test similar to that for the dialdehyde **4** was performed to determine the stability of the diphosphonate **9** in the presence of *t*-BuOK. The $^1$H NMR analysis showed that even after 35 min in the THF solution of large excess of *t*-BuOK, the diphosphonate remained intact (after acidic work up). As in the synthesis of the PPV donor block, a slight excess of **9** was used to ensure that the resulting acceptor blocks ($\mathbf{A_1}$ and $\mathbf{A_2}$) were end-capped with phosphonates. Because of the lower content of alkoxy side chains, the solubility of $\mathbf{A_2}$ is much poorer than that of $\mathbf{A_1}$, even though $\mathbf{A_2}$ is designed to be only half as long as $\mathbf{A_1}$. Again, the reactions were complete as evidenced by the disappearance of the aldehyde peaks in the $^1$H NMR spectra of $\mathbf{A_1}$ and $\mathbf{A_2}$ (in the Supporting Information). However, calculation of the ratio of phosphonate methylene protons (at the polymer ends) over aromatic protons becomes impossible because the weak methylene peaks (two doublets at 3.81 and 3.25 ppm from the sulfone monomer **8**) overlap with major peaks. Cis structures are also observed in the $^1$H NMR spectra.

**Synthesis of the Bridge Unit.** A literature procedure[21] was initially followed to prepare bridge compound **B** (structure shown in Scheme 3). However, the reaction between 1,2-dibromoethane and *p*-hydroxybenzaldehyde in refluxing acetone in the presence of potassium carbonate only afforded less than 10% of the product, much less than the reported 85%. A modified procedure using DMSO as solvent and NaOH as the base was used and a yield of 44% was obtained.

**Synthesis of the Block Copolymers.** A block copolymer of the type $(\mathbf{DBAB})_n$ can be synthesized by end-capping either a donor block or an acceptor block with the bridge unit to form aldehyde terminated **BDB** or **BAB** first, and then letting **BDB** or **BAB** react with phosphonate-end-capped acceptor block or donor block. In practice, we found that **BABs** were much less soluble than **A**s. On the contrary, the decrease in solubility from **D** to **BDB** is moderate. The $^1$H NMR spectrum of **BDB** is shown in Figure 2. The aldehyde peak from **B** is clearly seen. The integration ratio of the aldehydic proton peak and aromatic proton peaks is 1.80:142, very close to the designed ratio of 2:142. **DBD** was then allowed to react with $\mathbf{A_1}$ and $\mathbf{A_2}$ to produce the final block copolymer $(\mathbf{DBA_1B})_n$ and $(\mathbf{DBA_2B})_n$. At this last step, it is critical to heat the reaction mixture to dissolve the two PPV blocks as much as possible before the *t*-BuOK/THF solution was added to start the reaction. In the case of $\mathbf{BDB/A_1}$, it just took a couple of minutes of heating with a heat gun to dissolve the two precursors. The $^1$H NMR spectrum of $(\mathbf{DBA_1B})_n$ (Figure 3) shows that the aldehyde was completely gone. In the case of $\mathbf{BDB/A_2}$, there was always some amount of polymer (presumably $\mathbf{A_2}$ due to its poor solubility) remained undissolved and stuck to the side wall of the reaction flask. As a result, the block copolymer $(\mathbf{DBA_2B})_n$ still contained a significant amount of unreacted aldehyde as clearly shown in its $^1$H NMR spectrum (see Supporting Information). From the

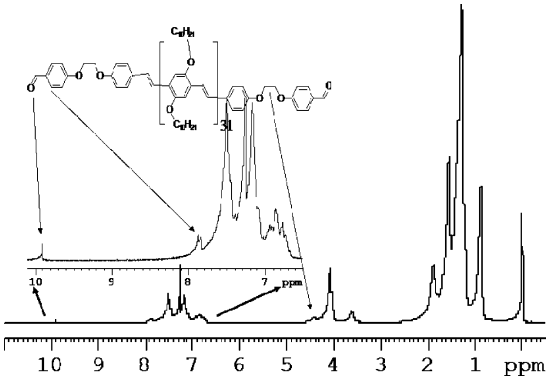

**Figure 2.** $^1$H NMR of **BDB** in $CDCl_3$. The inset spectrum shows the enlarged spectral region between 6.5 and 10.1 ppm. The integration ratio of the aldehydic proton and the aromatic protons (including vinylenic protons) is 1.84:142.

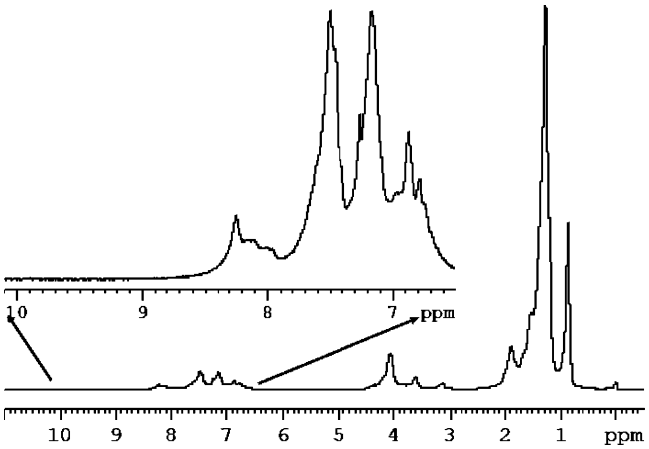

**Figure 3.** $^1$H NMR of $(\mathbf{DBA_1B})_n$ in $CDCl_3$. The aldehyde, which is present in the chemical structure and $^1$H NMR of **BDB**, is no longer seen here. Its disappearance is a direct evidence of the completeness of the reaction between **BDB** and $\mathbf{A_1}$.

**Table 1. Molecular Weights of Synthesized Polymers**

| | expected[a] $\bar{M}_n$ | $\bar{M}_w$ | $\bar{M}_n$ | $M_p$ | $\bar{M}_w/\bar{M}_n$ | M−H *a* |
|---|---|---|---|---|---|---|
| **D** | 13 131 | 23 K | 14 294 | 18 163 | 1.6 | 0.941 |
| $\mathbf{A_1}$ | 13 900 | 30 K | 15 724 | 20 364 | 1.9 | 0.786 |
| $\mathbf{A_2}$ | 5258 | 108 K | 9955 | 13 286 | 109 | 0.308 |
| $(\mathbf{DBA_1B})_n$ | 216 K | 204 K | 12 781 | 14 431 | 16 | 0.541 |
| $(\mathbf{DBA_2B})_n$ | 97 K | 120 M | 21 352 | 44 899 | 5600 | 0.237 |

[a] Expected $\bar{M}_n$ values are calculated based on monomer ratio described in the Experimental Section.

integrations of the aldehydic proton peak and aromatic proton peaks, the amount of $\mathbf{A_2}$ incorporated into the block copolymer is estimated to be roughly 48 mol %.

**Molecular Weight Measurement.** Molecular weights were measured by a Viscotek gel permeation chromatography (GPC) system equipped with a differential refractive index detector, a viscosity detector, and a light scattering detector. The universal calibration[24,25] with polystyrene standards was used to calculate the molecular weights. The results are shown in Table 1. For **D** and $\mathbf{A_1}$, both fully soluble in THF at room temperature at a concentration of 2 mg/mL, the measured molecular weights ($\bar{M}_n$) are very close to the calculated $\bar{M}_n$. The slightly larger values of measured $\bar{M}_n$ (by 8.8% and 13% for **D** and $\mathbf{A_1}$ respectively) are expected since a few percent of polymer products (presumably low molecular weights fractions) were lost in methanol during precipitation. However, for other polymers, because of limited solubility (only fully dissolved when heated at concentrations of 1−2 mg/mL in THF), aggregation cannot be avoided at the relatively high concentrations required for GPC measurement. As a result, GPC curves are broad and long tails are seen at the high molecular weight side of their GPC peaks, which give very high polydispersities for these polymers. In the case of $\mathbf{A_2}$, $\bar{M}_n$ is significantly higher than the calculated value. This can be attributed to two factors: (1) 34% of polymer, presumably rich of lower molecular weight fractions, was lost in the precipitation process, and (2) the formation of intermolecular aggregates has occurred. On the other hand, $\bar{M}_n$ values of block copolymers $(\mathbf{DBA_1B})_n$ and $(\mathbf{DBA_2B})_n$ are lower than expected. This can most probably be attributed to intramolecular folding of the polymer molecules (i.e., folding of rigid blocks onto each other), which is expected due to the existence of flexible bridge and low compatibility with the solvent. This folding will reduce the hydrodynamic radii of the polymers. The excessively high $\bar{M}_w$ of $(\mathbf{DBA_2B})_n$ (120 M) is attributed to intermolecular aggregation of this low solubility polymer. The aggregation behavior of $\mathbf{A_2}$, $(\mathbf{DBA_1B})_n$ and $(\mathbf{DBA_2B})_n$ are also reflected in their low *a* value in the Mark−Houwink empirical relationship[26] between polymer intrinsic viscosity $[\eta]$ and molecular weight $M$: $[\eta] = kM^a$ (see M−H *a* values in Table 1). Since *a* is normally a near zero for globular proteins, 0.5 (in poor solvents) or 0.8 (in good solvents) for coil molecules, or 1.0 or greater for extended rodlike molecules, the aggregation makes these polymers, particularly $(\mathbf{DBA_2B})_n$, behave more like globular proteins in THF.

**Absorption and Photoluminescence Spectra.** The absorption peak wavelengths, extinction coefficients, and photoluminescence peak wavelengths are listed in Table 2. (The UV−vis absorption spectra of the dilute chloroform solutions and thin films of the D and A blocks, their physical blends and block copolymers are provided in Supporting Information.) It is noted that the electron-withdrawing sulfone group blue shifts the absorption $\lambda_{max}$ (465 nm of $\mathbf{A_1}$ vs 483 nm of **D**), but causes no significant change in extinction coefficient ($5.60 \times 10^5$ L mol$^{-1}$cm$^{-1}$ for $\mathbf{A_1}$ vs $5.64 \times 10^5$ L mol$^{-1}$cm$^{-1}$ for **D**). Removal of electron-donating alkoxy groups from the system produces the major part of the absorption blue shift from 465 nm of $\mathbf{A_1}$ to 426 nm of $\mathbf{A_2}$ (the minor part is produced by the reduction in polymer length). In going from solution in chloroform to thin film, **D** exhibits a slight blue shift in absorption $\lambda_{max}$, while $\mathbf{A_1}$ and $\mathbf{A_2}$ exhibit red shifts of 9 nm and 6 nm, respectively. The different behavior can be explained by the change of the environment surrounding the PPV conjugate systems. Because **D** is nonpolar and has long hydrocarbon side chains, the environment of $\pi$-conjugate system of **D** in the solid state is actually less polar than that in the chloroform solution, and therefore causes a blue shift in the UV−vis absorption. On the other hand, the sulfone-substituted phenylene units in $\mathbf{A_1}$ and $\mathbf{A_2}$ are highly polar and likely provide more polar environments than chloroform.

Photoluminescence (PL) spectra of $\mathbf{A_1}$, $\mathbf{A_2}$, **D**, $(\mathbf{DBA_1B})_n$, and $(\mathbf{DBA_2B})_n$ in chloroform solutions are shown in Figure 4. $\mathbf{A_1}$ and $\mathbf{A_2}$ solutions were excited at their peak absorption wavelengths: $\mathbf{A_2}$, 426 nm; $\mathbf{A_1}$, 465 nm; **D**, $(\mathbf{DBA_1B})_n$ and $(\mathbf{DBA_2B})_n$ solutions were excited at **D**'s peak absorption wavelength: 483 nm. At 483 nm, $\mathbf{A_1}$ absorbance is slightly smaller than of that of **D** (by about 8%, from Figure 8 in the Supporting Information and Table 2), yet the PL of pristine $\mathbf{A_1}$ is much stronger than that of pristine **D** (by over 50%) (Figure 4a), the contribution from $\mathbf{A_1}$ to the overall PL from $(\mathbf{DBA_1B})_n$ solution should be relatively greater than that from **D**. The fact that the PL profile of $(\mathbf{DBA_1B})_n$ was dominated by **D** (Figure 4b) indicates a possible energy transfer from $\mathbf{A_1}$ to **D**. However, the overall

**Table 2. Optical Properties and Energy Levels of the Synthesized Polymers**

| | absorption $\lambda_{max}$ (nm) solution[a]/film | $e$ (L mol$^{-1}$ cm$^{-1}$) ($CHCl_3$) | $\lambda_{Em\ max}/\lambda_{Ex}$ (nm) ($CHCl_3$) | $\lambda_{Em\ max}$ (nm) (film) | $\Delta\lambda_{Em\ max}$ (nm) ($CHCl_3 \rightarrow$ film) | $\lambda_{abs\ cutoff}$ (nm/eV) (THF)[b] | LUMO/HOMO |
|---|---|---|---|---|---|---|---|
| **D** | 483/481 | $5.64 \times 10^5$ | 551/483 | 582 | 31 | 555/2.24 | −2.91/−5.15 |
| $\mathbf{A_1}$ | 465/474 | $5.60 \times 10^5$ | 541/465 | 612 | 71 | 533/2.33 | −3.15/−5.48 |
| $\mathbf{A_2}$ | 426/432 | $2.54 \times 10^5$ | 492/426 | 566 | 74 | 506/2.45 | −3.07/−5.52 |
| $\mathbf{D} + \mathbf{A_1}$ | −/477 | | 543/483 | 592, 624 | | | |
| $\mathbf{D} + \mathbf{A_2}$ | −/463 | | 550/483 | 584 | | | |
| $(\mathbf{DBA_1B})_n$ | 467/475 | | 550/483 | 592, 621 | | | |
| $(\mathbf{DBA_2B})_n$ | 458/455 | | 550/483 | 581 | | | |

[a] In $CHCl_3$. [b] THF solvent was used here because the cyclovoltametry was performed in THF.

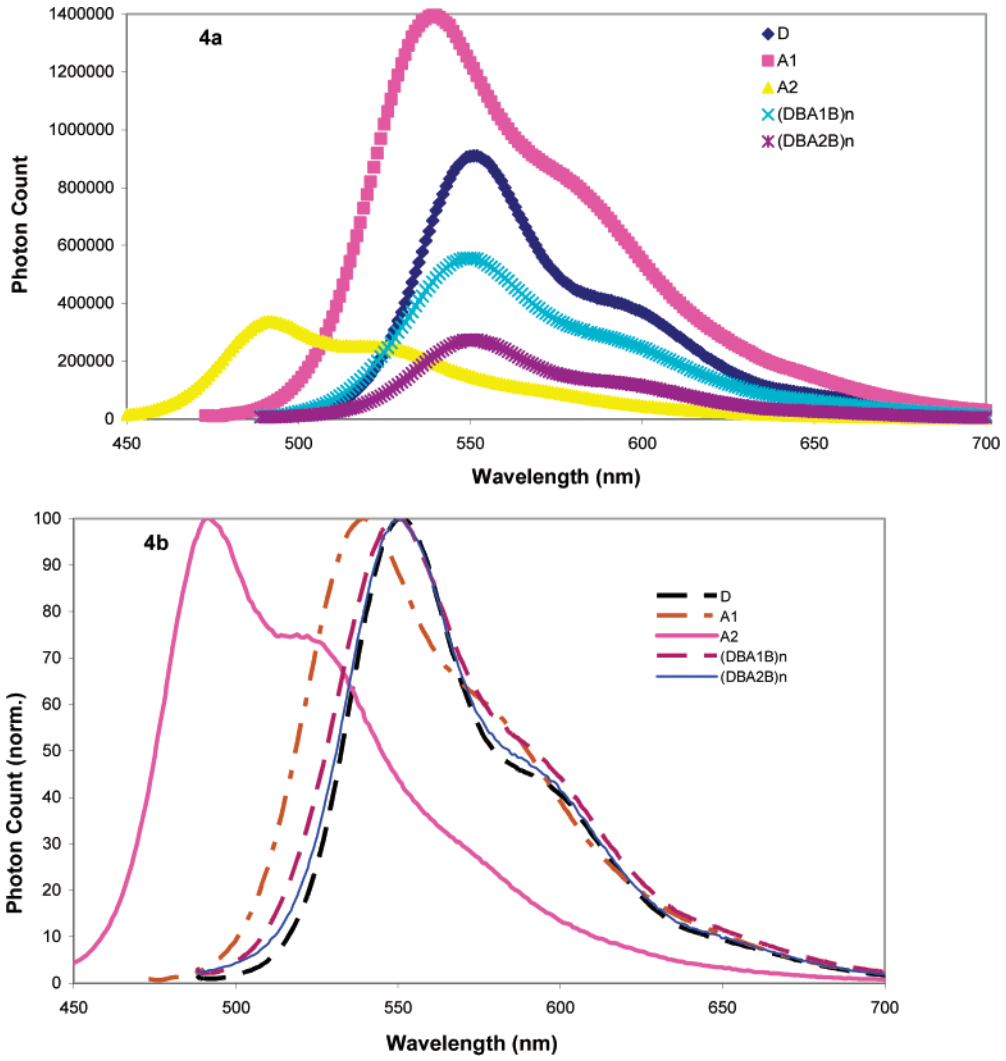


**Figure 4.** (a) Photoluminescence spectra of $\mathbf{A_1}$, $\mathbf{A_2}$, **D**, $(\mathbf{DBA_1B})_n$ and $(\mathbf{DBA_2B})_n$ in chloroform solutions. Molar concentrations are 10 nM for $\mathbf{A_1}$, $\mathbf{A_2}$, and **D** solutions, and are 5nM for the block copolymer solutions (making the total concentrations of **A** and **D** also 10 nM). Excitation wavelengths: $\mathbf{A_2}$, 426 nm; $\mathbf{A_1}$, 465 nm; **D**, $(\mathbf{DBA_1B})_n$ and $(\mathbf{DBA_2B})_n$, 483 nm. The peak PL intensity of $(\mathbf{DBA_2B})_n$ solution was only 30% of the PL of pristine **D** despite the concentration of D $(\mathbf{DBA_2B})_n$ solution is 50% of pristine **D**. The rest of the PL reduction (about 20%) can be explained by the charge transfer from **D** to $\mathbf{A_2}$. (b) Normalized version of 4a for a better comparison of PL spectrum profiles.

PL intensity of $(\mathbf{DBA_1B})_n$ is much smaller compared to the pristine **D** and $\mathbf{A_1}$, and this was presumably due to the electron transfer from the **D to** $\mathbf{A_1}$. In the case of $(\mathbf{DBA_2B})_n$, it is not surprising that the PL profile of $(\mathbf{DBA_2B})_n$ follows that of **D** closely, since $\mathbf{A_2}$ absorbs weakly at 483 nm. The overall PL emission intensity of $(\mathbf{DBA_2B})_n$ is much lower compared to the **D**, signifying the electron transfer from **D** to $\mathbf{A_2}$.

**HOMO/LUMO Energies and Donor/Acceptor LUMO Offsets.** The HOMO and LUMO energy levels were determined by cyclic voltammetry (CV) combined with UV−vis spectra. The excitation energy gaps of **D**, $\mathbf{A_1}$, and $\mathbf{A_2}$ were estimated from the onset of absorption peak of the UV−vis absorption peak in THF solution, and were 2.24, 2.33, and 2.45 eV respectively. CV was used to identify the HOMO level positions based on the correlation between oxidation potentials and the HOMO orbitals referenced to ferrocene. The HOMO values were found to be −5.15 eV, −5.48 eV, and −5.52 eV for **D**, $\mathbf{A_1}$, and $\mathbf{A_2}$ respectively. With the known energy gaps and HOMO values, the LUMO levels were calculated to be −2.91, −3.15, and −3.07 eV, respectively.

**Film Preparation and Aggregation Behaviors.** The solubilities of the materials in chloroform exhibit the following sequence: $\mathbf{A_1} > \mathbf{D} > (\mathbf{DBA_1B})_n > (\mathbf{DBA_2B})_n > \mathbf{A_2}$. $\mathbf{A_1}$ is fully soluble in polar solvents, such as 1,1,2-trichloroethane (TCE).

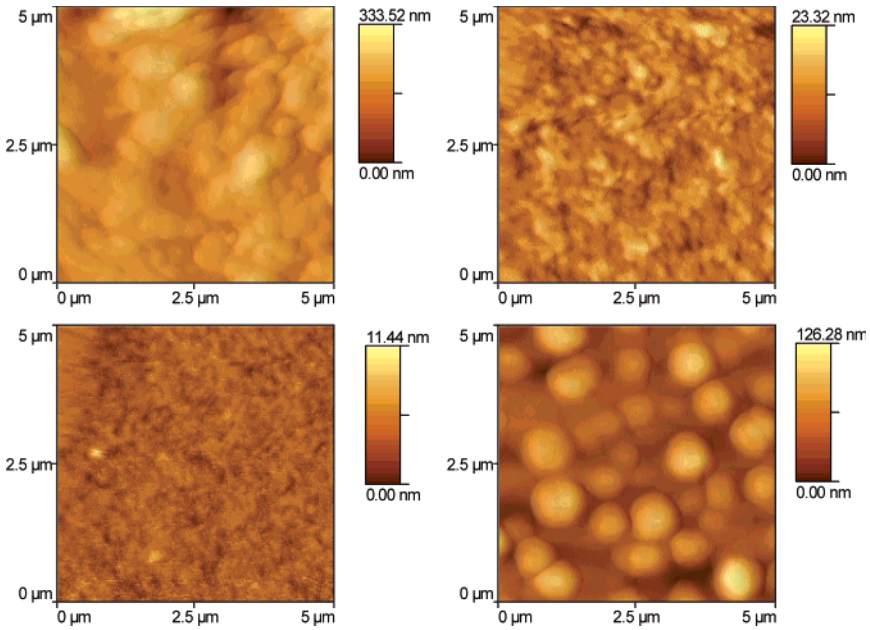


**Figure 5.** AFM topological images of donor and acceptor films spin-coated on glass slides: (a) (top left) **D**, room-temperature substrate; (b) (top right) **D**, preheated substrate; (c) (bottom left) $\mathbf{A_1}$, ambient temperature substrate; (d) (bottom right) $\mathbf{A_2}$, preheated substrate. Immediately before spin-coating, all polymer solutions in 1,1,2-trichloroethane, except the $\mathbf{A_1}$ solution (fully soluble at room temperature), were heated to 122 °C (the boiling point of the solvent) until the solutions became clear. Preheating of the glass substrates was done on a hot-plate with a surface temperature of 140 °C.

All other polymers were fully dissolved only at elevated temperatures. Hot filtration was necessary to pass the solution through 0.2 $\mu$m syringe filters. All of the filtered solutions, except $\mathbf{A_1}$, usually gel out within a few minutes. Preheating was done immediately before spin-coating to obtain a homogeneous solution. For this reason, high-boiling-point solvents, such as TCE and 1,2-dichlorobenzene, were used. Hot substrates (glass or ITO/glass) are used to prevent early precipitation of polymers, especially $\mathbf{A_2}$, on the surface of the substrates. When 1,2-dichlorobenzene was used as the solvent, the coated substrates were immediately brought to a hot plate so that the film would dry without severe aggregation of polymers.

It is critical to have physically different donor and acceptor blocks so that they will phase-separate in the thin film. The difference in their intermolecular interactions can be examined by studying their tendency of aggregation during the film forming process using tapping mode atomic force microscopy. The results are presented in Figure 5. It was found that $\mathbf{A_1}$ was the most processable polymer and formed optical quality film at room temperature. Its AFM topological image (Figure 5c) indicates a smooth surface without noticeable aggregation. **D** formed very hazy films when the coating of **D**/TCE was dried at room temperature. Its AFM topological image (Figure 5a) shows that the film was full of aggregates of the sizes of several hundreds nanometers. When a hot substrate was used, transparent films were obtained as a result of faster solvent evaporation. Large-size aggregates were not observed with AFM (Figure 5b). $\mathbf{A_2}$ formed aggregates up to 800 nm in size even when a hot substrate was used (Figure 5d). So, the aggregation tendencies ($\mathbf{A_2} > \mathbf{D} > \mathbf{A_1}$) of the three blocks correlate well with their solubility in organic solvents.

**Photoluminescence in Thin Films.** PL spectra of films composed of the donor, acceptors, their blends, and block copolymers are shown in Figure 6. As the PL spectral profiles are not sensitive to excitation wavelength as long as the wavelength is within interband absorption wavelength range (an example is given in the Supporting Information for $\mathbf{A_2}$),[27] the same excitation wavelength (481 nm) was used to excite all the samples. The PL peak wavelengths of **D**, $\mathbf{A_1}$, and $\mathbf{A_2}$ films are summarized in Table 2 along with the results in chloroform solutions. Both the donor and acceptor polymers exhibited red shifts in peak PL wavelength from solution to thin films. Interestingly, the red shifts of the two acceptor polymers are much bigger than that of the donor polymer. Similar differences were observed for poly[2-methoxy-5-(2′-ethylhexyloxy)phenylenevinylene] (MEH−PPV) and cyano-substituted poly(phenylenevinylene), CN−PPV.[27] In general, PL of polymers in the solid state is dominated by excited dimer emission, which is red shifted compared to that of a single-chain exciton by an amount depending on the interchain coupling. Calculations by Wu et al.[28] showed that the interchain coupling is much stronger in CN−PPV than in MEH−PPV, a result of smaller interchain distance in CN−PPV film, which was also predicted by calculation[29] and proved experimentally by Chen et al.[30] The stronger interchain interaction in CN−PPV was attributed to the presence of the electron-withdrawing cyano group. Similarly, the sulfone group in $\mathbf{A_1}$ and $\mathbf{A_2}$ is responsible for larger red-shift of PL in $\mathbf{A_1}$ and $\mathbf{A_2}$ thin films.

The thickness of all films from which the data in Figure 6 were acquired were all chosen to be greater than 90 nm, as we found that fluorescence intensities of the polymer films become thickness-independent beyond this thickness. Since the angle between the films and incident excitation beam was set at 42°, the effective thicknesses of all the films were above 180 nm, which is enough for the polymers to absorb essentially all the incident light. This thickness-independence allowed a rough comparison of PL quenching. Because the excitation wavelength is the peak wavelength of **D**, and $\mathbf{A_2}$ absorbs weakly at this wavelength, PL spectra of films of $\mathbf{D}/\mathbf{A_2}$ blend (1:1 molar) and $(\mathbf{DBA_2B})_n$ have the same profile as that of **D**, but with lower intensity. Relatively lower photoluminescence peak intensities of $\mathbf{D}/\mathbf{A_2}$ and $(\mathbf{DBA_2B})_n$ films as compared with that of film **D** were caused by partial quenching of the donor emission with a rate of 53% in the blend and 78% in the block copolymer due

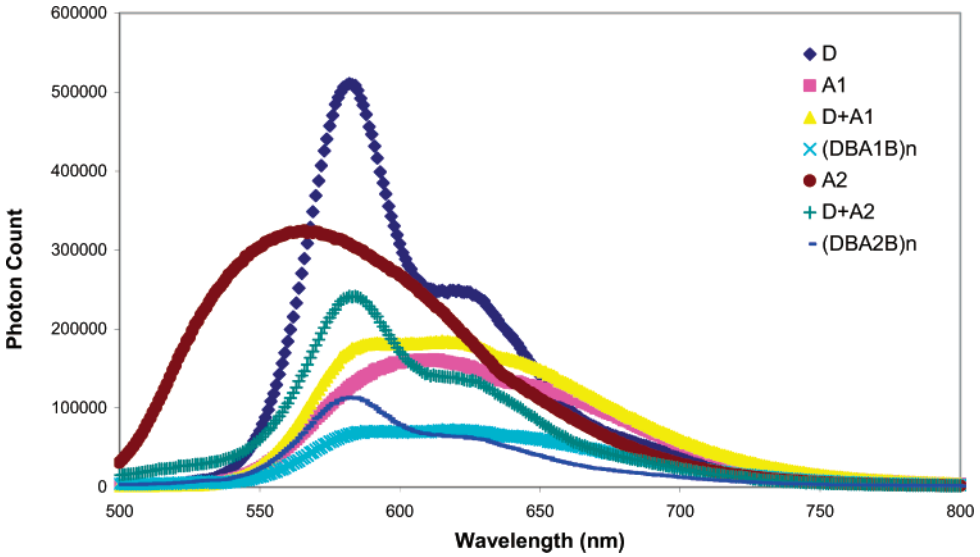


**Figure 6.** Photoluminescence spectra of thin films of **D**, $\mathbf{A_1}$, $\mathbf{D/A_1}$ (1:1 molar), $(\mathbf{DBA_1B})_n$, $\mathbf{A_2}$, $\mathbf{D/A_2}$ (1:1 molar), and $(\mathbf{DBA_2B})_n$. Excitation wavelength: 481 nm.

to the electron transfer from **D** to $\mathbf{A_2}$. However, this electron transfer does not appear to be complete due to insufficient energy difference between the LUMO levels of **D** and $\mathbf{A_2}$.[31] If integration of emitted photon in the range of 500 nm to 800 nm are used, the overall quenching rates are 41% in the blend and 73% in the block copolymer. The lower degree of PL quenching in the blend film is attributed to large scale phase separation of **D** and $\mathbf{A_2}$ due to difference in their aggregation tendency. Figure 7 shows AFM topographic images of the as-cast $(\mathbf{DBA_2B})_n$ and $\mathbf{D/A_2}$ blend films. The block copolymer film is much more uniform than the blend film. The islands on the surface of the blend film are believed to be the $\mathbf{A_2}$ domains since $\mathbf{A_2}$ aggregates much more readily that **D**.

Because of the smaller difference in energy gaps between **D** and $\mathbf{A_1}$ (as compared to that between **D** and $\mathbf{A_2}$) and the greater red shift of PL of $\mathbf{A_1}$ in solid state, the PL peak wavelength of $\mathbf{A_1}$ film appeared on the longer wavelength side of the donor polymer PL. Because the absorbance of $\mathbf{A_1}$ at the excitation wavelength (481 nm) is smaller than that of **D** by only ~5%, the PL profiles show the characteristics of both **D** and $\mathbf{A_1}$. Despite of relatively lower energy of excited state of $\mathbf{A_1}$ (in the form of excimer), the fact that the feature from $\mathbf{A_1}$ is not dominant in the profiles of both $(\mathbf{DBA_1B})_n$ and $\mathbf{D/A_1}$ PL spectra suggests that the net energy transfer from the excited state of **D** to $\mathbf{A_1}$ was insignificant. Fluorescence quenching rates, as calculated using the photon integration over the range of 500−800 nm, are 35% and 73% for $\mathbf{D/A_1}$ blend film and $(\mathbf{DBA_1B})_n$ film, respectively. Photoinduced charge separation has been observed and the photovoltaic device is under optimization.

## Conclusions

A novel class of PPV-based light harvesting conjugated block copolymers, with electron-donating conjugated blocks connected to the electron-accepting conjugated blocks via nonconjugated and flexible bridge units, have been designed, synthesized, and characterized. The optical excitation energy gaps are 2.24 eV for the donor block, 2.33 and 2.45 eV for the two acceptor blocks synthesized, with donor/acceptor LUMO energy offsets of 0.24 and 0.16 eV respectively. While GPC worked well for the soluble blocks **D** and $\mathbf{A_1}$, it gave excessively large molecular weights for less soluble polymer $\mathbf{A_2}$ and block copolymers $(\mathbf{DBA_1B})_n$ and $(\mathbf{DBA_2B})_n$ due to intermolecular aggregation. Despite the very large weight-average molecular weights ($M_w$), both block copolymers have relatively low GPC measured number-average molecular weights ($M_n$). This indicates the intramolecular folding of the PPV blocks in the block copolymers in THF solution.

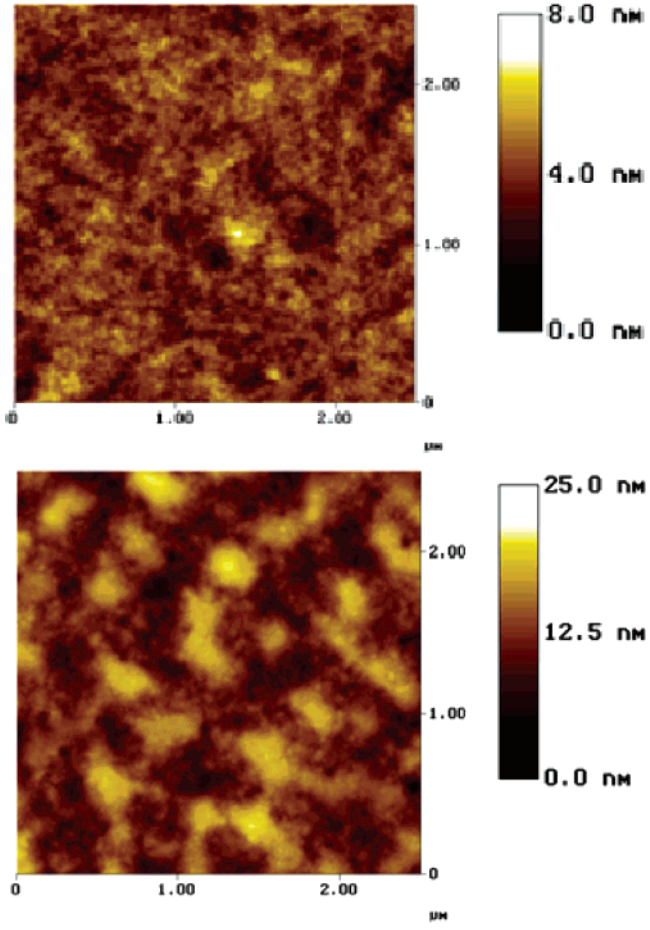


**Figure 7.** AFM topological images of as-cast $(\mathbf{DBA_2B})_n$ block copolymer (top) and $\mathbf{D/A_2}$ blend (bottom).

The two acceptor polymers exhibit very large red shifts (71 and 74 nm for $\mathbf{A_1}$ and $\mathbf{A_2}$ respectively) in photoluminescence peak wavelength from solution to thin film, more than twice as much as that observed for **D** (31 nm). The larger red shifts are attributed to the influence of sulfone electron-withdrawing

groups in $\mathbf{A_1}$ and $\mathbf{A_2}$ conjugated systems in a way similar to that of the cyano group in CN−PPV, which leads to stronger interchain interaction and hence formation of lower-energy excimers upon excitation.

The block copolymers exhibited better processability than the corresponding blends of individual blocks. More importantly, block copolymer does not have large scale phase separation problem as do the blends during film forming process, therefore, stronger photoluminescence quenching in block copolymers films were expected and indeed observed. Although the reaction for $(\mathbf{DBA_2B})_n$ preparation was not complete due to the relatively poor solubility of the $\mathbf{A_2}$ block, the existence of free $\mathbf{A_2}$ does not seem to have a detrimental effect on the film forming property and PL quenching rate of $(\mathbf{DBA_2B})_n$. This may suggest that block copolymer may be used as a binding agent to prevent large scale phase separation between the donor polymer and acceptor polymer. The methodology developed in this work could also be applied to the development of more promising systems, such as a DBA triblock copolymer which is more challenging in synthesis due to the need for a mono-end functionalized "end-capper" and a monomer with two different functional groups.

**Acknowledgment.** This work was supported, in part, by research and educational grants from a number of agencies, including NASA (Awards NCC3-1035 and NNC04GB67G), the Air Force Office of Scientific Research (Award F-49620-01-1-0485), and the National Science Foundation (Award HRD-0317722).

**Supporting Information Available:** Text detailing the decomposition product analysis (including figures showing the NMR spectra and structures of the compounds involved and a reaction scheme) of 2,5-bisdecyloxy-1,4-benzenedicaboxaldehyde (**4**) and figures showing $^1$H NMR spectra of $\mathbf{A_1}$, $\mathbf{A_2}$, and $(\mathbf{DBA_2B})_n$, UV−vis absorption spectra, cyclovoltamic scans of $\mathbf{A_1}$ and $\mathbf{A_2}$, and photoluminescence spectra of $\mathbf{A_1}$ with different excitation wavelengths. This material is available free of charge via the Internet at http://pubs.acs.org.

## References and Notes

(1) Tang, C. *Appl. Phys. Lett.* **1986**, *48*, 183.
(2) (a) Sun, S.; Sariciftci, N. *Organic Photovoltaics: Mechanisms, Materials and Devices*; CRC Press: Boca Raton, FL, 2005. (b) Hoppe, H.; Sariciftci, N. S. *J. Mater. Res.* **2004**, *19*, 1924−1945. (c) Coakley, K.; McGehee, M. *Chem. Mater.*. **2004**, *16*, 4533. (d) Brabec, C.; Dyakonov, V.; Parisi, J.; Sariciftci, N. *Organic Photovoltaics: Concepts and Realization*; Springer: Berlin, 2003.
(3) Sariciftci, S.; Zhang, C.; Heeger, A. J.; Wudl, F. *Appl. Phys. Lett.* **1993**, *62*, 585.
(4) Yu, G.; Gao, J.; Hummelen, J. C.; Wudl, F.; Heeger, A. J. *Science* **1995**, *270*, 1789.
(5) Halls, M.; Walsh, C.; Greenham, N.; Marseglla, E.; Friend, R.; Moratti, S.; Holmes, A. *Nature (London)* **1995**, *376*, 498.
(6) (a) Li, G.; Shrotriya, V.; Huang, J.; Yao, Y.; Moriarty, T.; Emery, K.; Yang, Y. *Nat. Mater.* **2005**, *4*, 864−868. (b) Ma, W.; Yang, C.; Gong, X.; Lee, K.; Heeger, A. *Adv. Funct. Mater.* **2005**, *15*, 1617−1622.
(7) (a) Hadjichristidis, N., Pispas, S., Floudas, G., Eds. *Block Copolymers: Synthetic Strategies, Physical Properties, and Applications*; John Wiley & Sons: New York, 2003. (b) Hamley, I. W. *The Physics of Block Copolymers*; Oxford University Press: Oxford, U.K., 1998. (c) Bates F. S.; Fredrickson, G. H. *Annu. Rev. Phys. Chem.* **1990**, *41*, 525−557.
(8) (a) Cravino, A.; Sariciftci, N. S. *J. Mater. Chem.* **2002**, *12*, 1931−1943. (b) Jousselme, B.; Blanchard, P.; Levillain, E.; de Bettignies, R.; Roncali, J. *Macromolecules* **2003**, *36*, 3020−3025.
(9) Giacalone, F.; Segura, J. L.; Martin, N.; Catellani, M.; Luzzati, S.; Lupsac, N. *Org. Lett.* **2003**, *5*, 1669−1672.
(10) Catellani, M.; Luzzati, Silv.a; Lupsac, N.-O.; Mendichi, R.; Consonni, R.; Famulari, A.; Meille, S. V.; Giacalone, F.; Segura, J. L.; Martin, N. *J. Mater. Chem.* **2004**, *14*, 67−74.
(11) (a) Stalmach, U.; de Boer, B.; Videlot, C.; van Hutten, P. F.; Hadziioannou, G. *J. Am. Chem. Soc.* **2000**, *122*, 5464−5472. (b) Boer, B.; Stalmach, U.; Hutten, P.; Melzer, C.; Krasnikov, V.; Hadziioannou, G. *Polymer* **2001**, *42*, 9097.
(12) (a) Sun, S.; Fan, Z.; Wang, Y.; Taft, C.; Haliburton, J.; Maaref, S. *Org. Photovoltaics II, SPIE* **2002**, *4465*, 121−128. (b) Fan, Z. Synthesis and Characterization of a Novel Block Copolymer System Containing RO−PPV and SF−PPV−I Conjugated Blocks. MS Thesis, Norfolk State University, 2002. (c) Wang, Y. Synthesis and Characterization of a New Acceptor (N-Type) Conjugated Polymer "SF−PPV−I". MS Thesis, Norfolk State University, 2002.
(13) Sun, S. *Sol. Energy Mater. Sol. Cells* **2003**, *79*, 257−264.
(14) Sun, S.; Fan, Z.; Wang, Y.; Haliburton, J. *J. Mater. Sci.* **2005**, *40*, 1429−1443.
(15) Jenekhe, S.; Chen, L. *Macromolecules* **1996**, *29*, 6189.
(16) Thomas, S.; Zhang, C.; Sun, S. *J. Polym. Sci., Polym. Chem.* **2005**, *43*, 4280−4287.
(17) Zhang, C.; Wang, C.; Dalton, L. R.; Sun, G.; Zhang, H.; Steier, W. H.; *Macromolecules* **2001**, *34*, 253−261.
(18) Sun, S.; Zhang, C.; Yang, Z.; Dalton, L. R.; Garner, S. M.; Chen, A.; Steier, W. H. *Polymer* **1998**, *39*, 4977−4981.
(19) Zhang, C. Unpublished results. Soluble PPV synthesis was conducted using the Horner−Emmons reaction in 2001−2002, and we found that soluble (alkoxy-derivatized) PPVs with $M_w$ of 60 000 could be synthesized from dialdehyde and diphosphonate monomers without formation of any cross-linked species.
(20) Wang, B.; Wasielewski, M. R. *J. Am. Chem. Soc.* **1997**, *119*, 12−21.
(21) Peumans, P.; Yakimov, A.; Forrest. S. R. *J. Appl. Phys.* **2003**, *93*, 3693−3723.
(22) Bao, Z.; Dodabalapur, A.; Lovinger, A. J. *Appl. Phys. Lett.* **1996**, *69*, 4108.
(23) Odian, G. *Principles of Polymerization*, 3rd ed.; Wiley: New York, 1991; p 79.
(24) Benoit, M.; Grubisic, F.; Rempp, R. *J. Polym. Sci., Part B:* **1967**, *5*, 753.
(25) www.viscotek.com.
(26) Yau, W. W.; Kirkland, J. J.; Bly, D. D. *Modern Size-Exclusion Liquid Chromatography;* John Wiley & Sons: New York, 1979.
(27) Harrison, N. T.; Baigent, D. R.; Samuel, I. D. W.; Friend, R. H.; Grimsdale, A. C.; Moratti, S. C.; Holmes, A. B. *Phys. Rev. B: Condens. Matter* **1996**, *53* (23), 15815−15822.
(28) Wu, M. W.; Conwell, E. M. *Phys. Rev. B: Condens. Matter* **1997**, *56*, R10060−R10062.
(29) Conwell, E. M.; Perlstein, J.; Shaik, S. *Phys. Rev. B: Condens. Matter* **1996**, *54*, R2308−R2310.
(30) Chen, S. H.; Su, C. H.; Su, A. C.; Chen, S. A. *J. Phys. Chem. B* **2004**, *108*, 8855−8861.
(31) Sun, S.-S. *Sol. Energy Mater. Sol. Cells* **2005**, *85*, 261−267.

MA060179J